Eigenfrequencies of a Truncated Conical Resonator via the Classical and Wentzel–Kramers–Brillouin Methods

Jonathan P. Van't Hof, *Member, IEEE*, and Daniel D. Stancil, *Fellow, IEEE*

***Abstract*—The eigenfrequencies within a truncated conical cavity resonator have similarities to the eigenfrequencies within both the cylindrical and spherical cavity resonators. This paper will first find the family of eigenfrequencies of the truncated conical cavity resonator by solving the classical boundary value problem in the spherical coordinate system, similar to a spherical cavity resonator. Next, eigenfrequencies for the truncated conical resonator are found via the cylindrical coordinate system using the Wentzel–Kramers–Brillouin (WKB) method by making the approximation that the truncated conical cavity with a small half-cone angle is a cylindrical cavity with linearly sloping walls. While the WKB method is an approximation to the actual eigenfrequencies, the solution yielded by this method is far more simple than the solution yielded by the classical boundary value method. Resonant frequencies are derived via both methods and are compared to each other and to measurements made in an experimental truncated conical cavity platform, displaying a very good agreement.**

***Index Terms*—Boundary value problems, cavity resonator filters, eigenvalues and eigenfunctions, microwave resonators, waveguides.**

Fig. 1. Truncated conical cavity resonator, shown with a meter stick for perspective.

I. Introduction

THE SOLUTIONS for the fields inside a truncated conical metallic cavity resonator are very similar to the solutions of the spherical cavity resonator, which are well known [1]. One of the key differences is the additional boundary conditions required to be imposed at the slanted sidewalls of the conical cavity resonator and the truncation of the cone at its small end. Fig. 1 shows a truncated conical cavity resonator with a fundamental resonance (TE_{111}) of 433 MHz. This particular experimental platform was used to characterize the communications channel that is the interior of electromagnetic resonant spaces, such as an aircraft wing or fuselage [2]–[5]. The platform's conical geometry reasonably simulated the tapering walls that one might find in an aircraft wing or fuselage, while also providing a semiregular geometry from which eigenvalues could be derived. A similar purely cylindrical platform was also utilized to characterize this communications channel.

Manuscript received December 19, 2007; revised March 10, 2008. First published July 25, 2008; last published August 8, 2008 (projected).

J. P. Van't Hof is with the Applied Physics Laboratory, The Johns Hopkins University, Laurel, MD 20723 USA.

D. D. Stancil is with the Department of Electrical and Computer Engineering, Carnegie Mellon University, Pittsburgh, PA 73015 USA.

Color versions of one or more of the figures in this paper are available online at http://ieeexplore.ieee.org.

Digital Object Identifier 10.1109/TMTT.2008.927408

Solutions for the truncated conical cavity resonator have been previously considered in the spherical coordinate system in [6], where investigators pursued a truncated conical resonator to test the conductivity of several superconducting thin films by measuring the quality factor of the TE_{011} mode. Solutions for this specific mode were presented, along with charts comparing the resonant frequencies of several mode families as functions of the cone length, width, and half-cone angle. Solutions for the truncated conical cavity resonator that proceed in the spherical coordinate system can be quite tedious and require the use of sophisticated mathematical tools, such as MATLAB[1] and Mathematica[2] to find the allowable noninteger degrees of the associated Legendre functions and to find the eigenvalues of noninteger order spherical Bessel functions.

The solutions for the eigenfrequencies in a truncated conical resonator with a small half-cone angle are also very similar to the eigenfrequencies inside a cylindrical cavity resonator. In a cylindrical waveguide, the propagation constant is the same for all points along the length of the waveguide (e.g., along the z-axis). However, a slight taper in the diameter of

[1]Product of The MathWorks Inc., Natick, MA. [Online]. Available: www.mathworks.com

[2]Product of Wolfram Research Inc., Champaign, IL. [Online]. Available: www.wolfram.com

the cylindrical waveguide along the z-axis gives the cylindrical guide a conical shape, and this taper can be seen as the propagation constant taking on a z-dependence. A method known to the quantum physics and microwave communities, the Wentzel-Kramers-Brillouin (WKB) approximation method, has often been utilized to solve differential equations with similar dependences on the differential variable. With respect to the truncated conical resonator, the WKB method can be used to derive a simple transcendental equation whose solutions give the resonant frequencies of an arbitrary mode. This method involves only trigonometric functions, and it requires only the zeros of the integer-order Bessel functions of the first kind and of its derivative, which are readily available in the form of tables [7]. Resonant solutions for the truncated conical resonator using the WKB method thus require considerably less sophisticated tools than the corresponding solutions in the spherical coordinate system, which demand the solution of noninteger order spherical Bessel functions and noninteger degree Legendre functions.

This paper will describe in detail two methods that can be used to find the resonant frequencies of a truncated conical cavity resonator. The resonant frequencies that are obtained from both the classical Legendre/Bessel eigenvalue method, from the WKB method and from measurements of the physical conical cavity resonator shown in Fig. 1, will be compared and a very close match among the three methods will be demonstrated. Even though the methods used to predict the eigenfrequencies of a conical cavity resonator can be applied to any arbitrary truncated cone resonator, the specific physical resonator shown in Fig. 1 will be considered so that empirical measurements of the resonant frequencies—found by measuring the frequency transfer function of the resonator using a vector network analyzer (VNA)—can be compared to the theoretical eigenfrequency predictions.

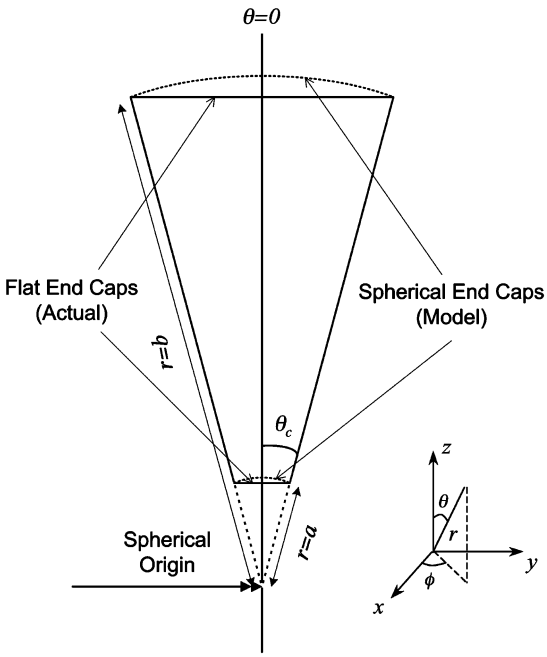

Fig. 2. Geometry in the spherical coordinate system (in the $\hat{\theta} - \hat{r}$ plane) for the conical resonator, showing the actual and modeled end caps at $r = a$ and $r = b$.

TABLE I
SPECIFICATIONS FOR THE TRUNCATED CONICAL CAVITY RESONATOR

PARAMETER	VALUE
Axial Length:	1.524 m (60 in.)
Small Diameter:	0.1143 m (4.5 in.)
Large Diameter:	0.5563 m (21.9 in.)
Half-cone Angle:	8.25°
Segments:	5
Material:	3.175 mm (0.125 in.) Al.
Fundamental Resonance:	TE_{111} @ 433 MHz

II. FIELD FUNCTIONS AND EIGENFREQUENCIES VIA THE CLASSICAL METHOD

The conical cavity resonator has the same underlying field solutions as a spherical resonator with additional boundary conditions at the small end cap ($r = a$) and the slanted walls ($\theta = \theta_c$), as shown in Fig. 2. The boundary conditions $\hat{n} \times \bar{E} = 0$ and $\hat{n} \cdot \bar{H} = 0$ (where $\hat{n}$ is the normal vector at any point on the cavity walls) must be satisfied on the outer end cap ($r = b$), the inner end cap, and the slanted walls. The classical solution for the cone begins by assuming that the projected center of the cone is at the origin of the spherical coordinate system. Although field and eigenfrequency solutions will be pursued for a general truncated conical resonator, the specific resonant frequencies derived will be for the geometry shown in Fig. 1 and summarized in Table I. For this geometry, the radial location of the small and large end caps are $r = a = 0.3983$ m and $r = b = 1.938$ m, respectively. The end caps of the geometry shown in Fig. 1 are flat—a fact that should be kept in mind throughout the upcoming discussions since the conical resonator in the spherical coordinate system assumes that the end caps are spherically rounded, as shown in Fig. 2.

The field functions for both the TM and TE polarizations can be derived from the following spherical coordinate mode functions [1]:

$$\psi_{mnp}^{\mathrm{TM}}(r,\theta,\phi) = \hat{B}_\nu\left(\frac{w'_{np}r}{a}\right) P_\nu^m(\cos\theta)\begin{Bmatrix}\cos m\phi\\ \sin m\phi\end{Bmatrix} \quad (1)$$

$$\psi_{mnp}^{\mathrm{TE}}(r,\theta,\phi) = \hat{B}_\nu\left(\frac{w_{np}r}{a}\right) P_\nu^m(\cos\theta)\begin{Bmatrix}\cos m\phi\\ \sin m\phi\end{Bmatrix}. \quad (2)$$

In the above expressions, $\hat{B}_\nu(x)$ is the νth-order spherical Bessel function (used by Schelkunoff [8]), and w_{np} and w'_{np} are the pth roots of the nth allowable order (given by the set of allowable orders ν) of these spherical Bessel functions and their first derivatives, respectively. $P_\nu^m(x)$ is the mth-order νth degree associated Legendre function of the first kind. In order to apply the boundary conditions, the field solutions must be produced from the mode functions in (1) and (2).

A. TM Field Functions and Boundary Conditions

Using (1) as the governing mode function, a vector potential expansion such as that outlined in [1] can be used to find the

complete electric and magnetic field functions for the TM polarization. The electric field functions are expressed as follows:

$$E_r = \frac{H_0}{j\omega\epsilon}\left(\omega^2\mu\epsilon + \frac{\partial^2}{\partial r^2}\right)\hat{B}_\nu\left(\frac{w'_{np}r}{a}\right) \cdot P_\nu^m(\cos\theta)\begin{Bmatrix}\cos m\phi\\ \sin m\phi\end{Bmatrix} \tag{3}$$

$$E_\theta = \frac{H_0}{j\omega\epsilon r}\frac{\partial}{\partial r}\hat{B}_\nu\left(\frac{w'_{np}r}{a}\right) \cdot \frac{\partial}{\partial\theta}P_\nu^m(\cos\theta)\begin{Bmatrix}\cos m\phi\\ \sin m\phi\end{Bmatrix} \tag{4}$$

$$E_\phi = H_0\frac{m}{j\omega\epsilon r\sin\theta}\frac{\partial}{\partial r}\hat{B}_\nu\left(\frac{w'_{np}r}{a}\right) \cdot P_\nu^m(\cos\theta)\begin{Bmatrix}-\sin m\phi\\ \cos m\phi\end{Bmatrix}. \tag{5}$$

The corresponding magnetic field functions can be found using Maxwell's equations. Enforcing the boundary condition that $E_\phi(r,\theta,\phi)|_{\theta=\theta_c} = 0$ for all ϕ and r in the cavity, we see that the following expression must be true:

$$P_\nu^m(\cos\theta)|_{\theta=\theta_c} = 0. \tag{6}$$

This boundary condition will be enforced by choosing the appropriate combinations of m and ν.

Enforcing the boundary condition that $E_\phi(r,\theta,\phi)|_{\substack{r=a\\r=b}} = 0$ results in the following condition to be true:

$$\frac{\partial}{\partial r}\hat{B}_\nu\left(\frac{w'_{np}r}{a}\right)\bigg|_{\substack{r=a\\r=b}} = 0. \tag{7}$$

The function $\hat{B}_\nu(x)$ is a linear combination of two functions that are solutions to Bessel's differential equation in spherical coordinates

$$\hat{B}_\nu(x) = \alpha\hat{J}_\nu(x) + \beta\hat{N}_\nu(x) \tag{8}$$

where $\hat{J}_\nu(x)$ is the spherical Bessel function of the first kind, $\hat{N}_\nu(x)$ is the spherical Bessel function of the second kind, and α and β are constants. These spherical Bessel functions can be related to the cylindrical Bessel functions, $J_\nu(x)$ and $N_\nu(x)$, via expressions given in [1].

Since the partial derivative with respect to r, as expressed in (7), must be zero when $r = a$ and $r = b$ in order to satisfy the $E_\phi = 0$ boundary condition, the constants α and β in (8) must be chosen such that the same choice of the eigenvalue $k'_r = w'_{np}/a$ causes the boundary condition to be enforced at both $r = a$ and $r = b$. Accordingly, if $\alpha = 1$ and $\beta = -(\hat{J}'_\nu(w'_{np}))/(\hat{N}'_\nu(w'_{np}))$, the boundary conditions at $r = a$ will be enforced independent of the value of $k'_r = w'_{np}/a$, where $\hat{J}'_\nu(x)$ and $\hat{N}'_\nu(x)$ are the derivatives of the first- and second-kind spherical Bessel functions. This choice for α and β leaves $k'_r = w'_{np}/a$ free to choose so that the boundary condition at $r = b$ is enforced. Thus, $\hat{B}_\nu((w'_{np}r)/(a))$ in the TM field functions is expanded as

$$\hat{B}_\nu\left(\frac{w'_{np}r}{a}\right) = \left[\hat{J}_\nu\left(\frac{w'_{np}r}{a}\right) - \frac{\hat{J}'_\nu(w'_{np})}{\hat{N}'_\nu(w'_{np})}\hat{N}_\nu\left(\frac{w'_{np}r}{a}\right)\right]. \tag{9}$$

B. TE Field Functions and Boundary Conditions

In the similar fashion as was done for the TM polarization, the governing mode function in (2) can be used with a vector potential expansion according to [1] to produce the complete electric and magnetic field expressions for the TE polarization. They can also be found using the TM field functions and the duality principle. For the purpose of brevity, only the E_ϕ electric field component is presented as follows, as the boundary conditions will be applied to it so that eigenvalues may be determined:

$$E_\phi = \frac{E_0}{r}\hat{B}_\nu\left(\frac{w_{np}r}{a}\right)\cdot\frac{\partial}{\partial\theta}P_\nu^m(\cos\theta)\begin{Bmatrix}\cos m\phi\\ \sin m\phi\end{Bmatrix}. \tag{10}$$

One can see from the above expression that in order for the boundary condition $E_\phi(r,\theta,\phi)|_{\theta=\theta_c} = 0$ to be true, the following restriction must be observed by choosing the Legendre orders m and degrees ν appropriately:

$$\frac{\partial}{\partial\theta}P_\nu^m(\cos\theta)\bigg|_{\theta=\theta_c} = 0. \tag{11}$$

To enforce the boundary condition that $E_\phi(r,\theta,\phi)|_{\substack{r=a\\r=b}} = 0$, the tentative expression for E_ϕ in (10) suggests that the following must be true:

$$\hat{B}_\nu\left(\frac{w_{np}r}{a}\right)\bigg|_{\substack{r=a\\r=b}} = 0 \tag{12}$$

where $\hat{B}_\nu(x)$ is the spherical Bessel function equal to a linear combination of the first- and second-kind spherical Bessel functions, as in (8). Similar to the TM solutions, if we let $\alpha = 1$ and $\beta = -(\hat{J}_\nu(w_{np}))/(\hat{N}_\nu(w_{np}))$, then E_ϕ will automatically be zero at $r = a$; the eigenvalue $k_r = w_{np}/a$ can then be chosen to make $E_\phi = 0$ additionally at $r = b$, satisfying the boundary conditions on all walls for the TE polarization fields. Thus, $\hat{B}_\nu((w_{np}r)/(a))$ in the TE field functions is expanded as

$$\hat{B}_\nu\left(\frac{w_{np}r}{a}\right) = \left[\hat{J}_\nu\left(\frac{w_{np}r}{a}\right) - \frac{\hat{J}_\nu(w_{np})}{\hat{N}_\nu(w_{np})}\hat{N}_\nu\left(\frac{w_{np}r}{a}\right)\right]. \tag{13}$$

These results reduce to and match the results obtained for the TE_{011} mode in [6] where investigators solved for the conical TE_{011} mode (because of its desirable current patterns) to investigate the conductivity of some superconducting films.

C. Eigenfrequencies

Through the process of applying the boundary conditions to obtain the field solutions, one can already begin to see how the eigenfrequencies are derived for the conical cavity. The boundary condition $E_\phi(r,\theta,\phi)|_{\theta=\theta_c} = 0$ for both the TM and TE polarizations restricts the choice of m and ν via (6) and (11). The Legendre function orders m are chosen from the set of integers ($m = 0, 1, 2, 3, \ldots$). For each order m, the noninteger Legendre degrees ν are found in order to satisfy (6) and (11), restricting the search to $\nu > m$ since $P_\nu^m(x) = 0$ for $\nu < m$ [1]. There are an infinite number of allowable degrees ν for each order m of the Legendre function, which is also infinite in number. Since the equations involving Legendre functions of noninteger degree do not have a closed-form solution, the

allowable degree in each chosen order must be found transcendentally, evaluating (6) and (11) using a root-finding algorithm in a computational tool such as Mathematica. The first root degree ν greater than m is represented with mode index triplet $(m, n = 1, p)$, the second with $(m, n = 2, p)$, and so forth.

One can see by examining the field functions of either polarization that the allowable degrees of the Legendre function become the allowable orders of the spherical Bessel functions. The first value of w'_{np} or w_{np} that causes the conditions in (7) and (12) to be true for the nth allowable order of the spherical Bessel function is given by the mode triplet with $p = 1$, the second with $p = 2$, and so forth. As with equations involving the Legendre function of noninteger degree, equations involving noninteger-order Bessel functions do not have closed-form solutions, and a transcendental equation must be solved using a computational tool to find the required roots. Once the eigenvalues $k_r = (w_{np})/(a)$ and $k'_r = (w'_{np})/(a)$ of the spherical Bessel functions are known, the resonant frequencies of the conical resonator quickly follow for the TM and TE polarization modes [1]

$$f_r^{\mathrm{TM}}(m,n,p) = \frac{\upsilon}{2\pi}\frac{w'_{np}}{a} \tag{14}$$

$$f_r^{\mathrm{TE}}(m,n,p) = \frac{\upsilon}{2\pi}\frac{w_{np}}{a} \tag{15}$$

where υ is the speed of light in the medium contained in the cavity. Note that the conical resonator still exhibits a degeneracy in the $\hat{\phi}$ dimension (except for the $m = 0$ index modes), given by the dual sine and cosine function options in TM and TE field functions. The fundamental resonance for the conical cavity is the TE_{111} mode ($\nu = 12.312$ and $w_{np} = 3.616$ for the cavity in Fig. 2), and its resonance frequency as given by (15) is 433.5 MHz.

The frequency response of the conical cavity resonator shown in Fig. 2 was measured by inserting two probes approximately 10 mm in length through the cavity walls near the large end $(r = b)$ of the cone and connecting one to each of the two ports of the network analyzer. Short probes were desired so that the cavity resonances were not substantially altered by the insertion of the probes themselves. As will be described later in this paper, some modes will cutoff as the radius of the cone gets progressively smaller, and so the insertion of the probes near the large end is important so that the low-order modes are not cutoff. The measured S_{21} response is shown in Fig. 3 with vertical dashed-line labels added to indicate where the theory outlined above predicts resonances. The roots of the spherical Bessel function are found using a root finding algorithm in MATLAB according to (7) and (12). One can see that the fit between the predicted value and the measured value is very good, and the errors are likely due, in part, to the assumption in the theoretical analysis that the end caps are rounded in shape—the actual end caps are flat.

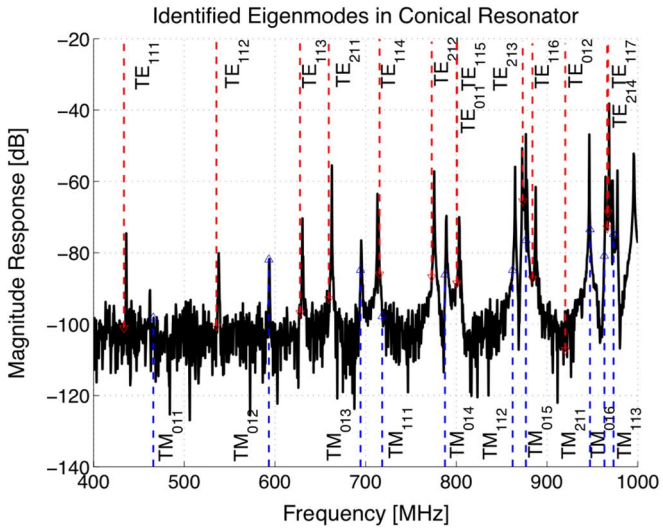

Fig. 3. Magnitude S_{21} response measured in the conical cavity resonator from 400 MHz to 1.0 GHz. Dashed lines and labels represent eigenfrequency predictions found by solving for the Legendre/Bessel eigenvalues.

III. EIGENFREQUENCIES VIA THE WKB METHOD

The transcendental solution of finding the eigenfrequencies for the conical resonator using the relations given in (6), (7), (11), and (12) can be very tedious, and requires some fairly advanced mathematical tools, such as Mathematica and MATLAB. An easier solution to find the resonant frequencies of the conical resonator is to utilize the WKB method, which has been applied to problems in quantum mechanics (e.g., [9]–[11]), optics, (e.g., [12]) and microwave electromagnetics (e.g., [13]–[16]). The authors of [14]–[16] applied the WKB method to conical waveguides, specifically to find the impedance of flared horn radiators. Though [14] showed that the limitation of the WKB method at its turning point causes certain inaccuracies in the solution for the impedance of flared horns, the same limitation does not appear to substantially impact the solution of the truncated conical resonator eigenfrequencies. As will be presented at the end of this section, the resonant frequencies of the truncated conical cavity resonator produced by the WKB method agree very well with classical and measured results.

A. WKB Approximation Method

The WKB method, in short, provides a method to find approximate solutions to a differential equation of the form

$$\frac{d^2y}{dx^2} + f(x)y = 0. \tag{16}$$

Notice that this differential equation has the same form as the wave equation in a particular dimension u

$$\frac{d^2\psi(u)}{du^2} + k_u^2(u)\psi(u) = 0. \tag{17}$$

The WKB solution assumes that $k_u^2(u)$ is no longer a constant, but is rather a slowly varying function over some dimension u. Making the transformation $y = e^{j\phi(x)}$, (16) becomes

$$-(\phi')^2 + j\phi'' + f(x) = 0. \tag{18}$$

If we assume that ϕ'' is small, then $\phi' = \pm\sqrt{f(x)}$ and $\phi = \pm\int\sqrt{f(x)}dx$. The WKB method specifies that in order for

$f(x)$ to be slowly varying, it must obey the following inequality [9]:

$$\frac{1}{2}\left|\frac{f'(x)}{\sqrt{f(x)}}\right| \ll |f(x)|. \tag{19}$$

From the differential expression in (16), it is known that if $f(x) < 0$, the solutions to the equation will be in the form of a decaying or growing exponential, and if $f(x) > 0$, the solutions will be harmonic functions, i.e., a linear combination of sines and cosines. If we let $f(x) < 0$ for $x < x_0$ and $f(x) > 0$ for $x > x_0$ and assume that the solution for $x < x_0$ must be of the decaying exponential form, the WKB method gives the solution to (16) as [9]

$$\frac{2}{\sqrt[4]{f(x)}}\cos\left[\int_{x_0}^{x}\sqrt{f(x')}dx' - \frac{\pi}{4}\right]. \tag{20}$$

Notice from this expression that the solutions to the WKB method will be oscillatory for $f(x) > 0$ and exponential for $f(x) < 0$.

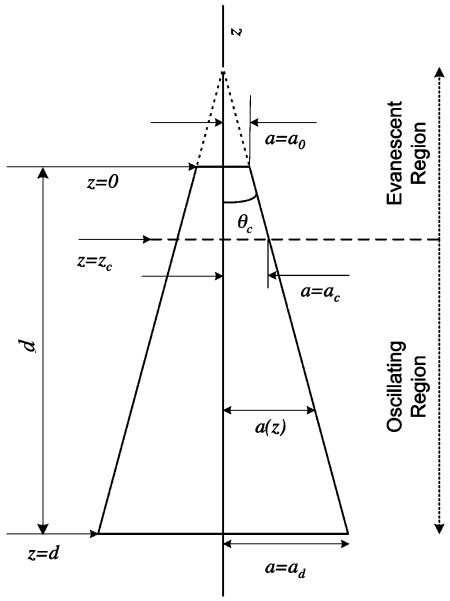

Fig. 4. Cross-sectional diagram of the geometry used to apply the WKB method in the conical resonator.

B. Applying the WKB Method to the Conical Cavity Resonator

Consider now the wave equation (Helmholtz equation) in cylindrical coordinates, whose solution for a longitudinal component of the electric or magnetic field is assumed to be of the product form $E_z(\rho,\phi,z) = R(\rho)\Phi(\phi)Z(z)$. Substitution of this product solution into the cylindrical Helmholtz equation and dividing by the same assumed solution yields

$$\frac{1}{\rho R(\rho)}\frac{d}{d\rho}\left(\rho\frac{dR(\rho)}{d\rho}\right) + \frac{1}{\rho^2\Phi(\phi)}\frac{d^2\Phi(\phi)}{d\phi^2} + \frac{1}{Z(z)}\frac{d^2Z(z)}{dz^2} + k^2 = 0 \tag{21}$$

which can be separated into three differential equations, one for each dimension in the cylindrical coordinate system. The differential expression for the $\hat{z}$-dimension is

$$\frac{d^2Z(z)}{dz^2} + k_z^2 Z(z) = 0 \tag{22}$$

which is of the form of (16), and k_z^2 is analogous to $f(x)$. Separation of (21) into each dimensional component leads to the dispersion relationship $k^2 = k_\rho^2 + k_z^2$. It can be seen that k_z^2 is a constant for a cylindrical cavity since $k^2 = \omega^2\mu\epsilon$ and $k_\rho^2 = (x_{np}/a)^2$, where x_{np} is the pth zero of the governing nth-order cylindrical Bessel function of the first kind (or its derivative, whose zero is represented as x'_{np}), and a is the radius of the cylindrical cavity resonator, which is constant over the length of a cylindrical resonator.

Now imagine that the radius of the cylindrical resonator is not a constant, but rather is a linearly varying parameter with z so the cavity takes on a truncated conical shape. According to the cross-sectional diagram shown in Fig. 4, the radius of the cavity can be written as $a(z) = a_0 + z\tan\theta_c$, where a_0 is the radius at $z = 0$ and θ_c is the half-cone angle of the right-angle cone. Substituting this expression for the radius into the cylindrical dispersion relation and solving for k_z gives

$$k_z(z) = \sqrt{k^2 - \left(\frac{x_{np}}{a_0 + z\tan\theta_c}\right)^2} = \sqrt{k^2 - k_\rho^2(z)}. \tag{23}$$

As is well known in waveguides, if $k_z^2 > 0$ (i.e., $k^2 > k_\rho^2$) the solutions to (22) will be the harmonic functions (modes resonate in the cavity). In contrast, if $k_z^2 < 0$ (i.e., $k^2 < k_\rho^2$), the solutions to (22) will be the growing and decaying exponentials (the resonant modes are cutoff and the fields evanesce in the cavity). The radius at which $k^2 = k_\rho^2$ can then be called the cutoff radius and is given by $a_c = x_{np}/k$ for a given mode with wavenumber k. Thus, modes in this quasi-cylindrical conical resonator whose eigenvalues are associated with x_{np} (or x'_{np}) will oscillate for radii greater than a_c and will evanesce for radii less than a_c. This cutoff radius can be solved for an equivalent point along the z-axis, $z_c = (a_c - a_0)/(\tan\theta_c)$. This point is called the turning point: the point at which propagating energy in the resonator turns back and propagates in the opposite direction, as if it were reflected. Since k_z^2 is now defined as a function of z, and z_c is the boundary between the exponential-solution region and the harmonic-solution region (analogous to x_0 in the above discussion of the WKB method), one can see that the fields in the quasi-cylindrical conical resonator have the same form as the expressions in (20) and that the WKB method can be applied to find an approximate solution for (22).

Since metallic waveguides and resonators have two sets of field solutions—one whose electric fields are transverse to the propagation direction (TE polarization) and the other whose magnetic fields are transverse to the propagation direction (TM

polarization)—it needs to be determined which of these solutions corresponds to the solution in (20). Consider the $\hat{\phi}$ component of the electric field (E_ϕ) for both the TM and TE field solutions in the cylindrical waveguide of radius a [1]

$$E_\phi^{\mathrm{TM}}(\rho,\phi,z) = \pm E_0 \frac{nk_z}{\omega\epsilon\rho} J_n\left(\frac{x_{np}\rho}{a}\right) \cdot \begin{Bmatrix} -\cos n\phi \\ \sin n\phi \end{Bmatrix} e^{\mp jk_z z} \tag{24}$$

$$E_\phi^{\mathrm{TE}}(\rho,\phi,z) = E_0 \frac{x'_{np}}{a} J_n\left(\frac{x'_{np}\rho}{a}\right) \cdot \begin{Bmatrix} \sin n\phi \\ \cos n\phi \end{Bmatrix} e^{\mp jk_z z}. \tag{25}$$

The total E_ϕ field is a superposition of the two propagating wavefronts $AE_\phi^- e^{jk_z z} + BE_\phi^+ e^{-jk_z z}$, where E_ϕ^- and E_ϕ^+ are, respectively, the reverse and forward propagating non-z components of E_ϕ expressed in (24) and (25). If perfectly reflecting end caps are placed at the points $z = 0$ and $z = d$ along the z-axis, it would be required that $E_\phi^{\mathrm{TM}}(z = 0) = E_\phi^{\mathrm{TM}}(z = d) = 0$ in (24) for the TM modes. Accordingly, $k_z = (q\pi)/(d)$ (where $q = 1, 2, 3, \ldots$) and $A = B$ in the above superposition, producing a standing wave proportional to $\sin(k_z z)$. Likewise, the boundary conditions on $E_\phi^{\mathrm{TE}}(z = 0) = E_\phi^{\mathrm{TE}}(z = d) = 0$ in (25) require that $k_z = (q\pi)/(d)$ and $A = -B$, also creating a superposition of the two waves that is proportional to $\sin(k_z z)$ for the TE modes.

The WKB solution, however, operates on the $\hat{z}$-field components in the cylindrical coordinate system, whose propagating wavefronts are reproduced as follows [1]:

$$E_z^{\mathrm{TM}}(\rho,\phi,z) = \frac{E_0}{j\omega\epsilon} J_n\left(\frac{x_{np}\rho}{a}\right) \begin{Bmatrix} \sin n\phi \\ \cos n\phi \end{Bmatrix} \cdot \left(\omega^2\mu\epsilon - k_z^2\right) e^{\mp jk_z z} \tag{26}$$

$$H_z^{\mathrm{TE}}(\rho,\phi,z) = \frac{E_0}{j\omega\epsilon} J_n\left(\frac{x'_{np}\rho}{a}\right) \begin{Bmatrix} \sin n\phi \\ \cos n\phi \end{Bmatrix} \cdot \left(\omega^2\mu\epsilon - k_z^2\right) e^{\mp jk_z z}. \tag{27}$$

The boundary requirements for the forward and reverse propagating waves found using the E_ϕ fields above ($A = B$ for TM and $A = -B$ for TE) must also apply to the other field components of each polarization in the resonator, including the $\hat{z}$ components in (26) and (27). Thus, given that $A = B$ for the TM modes, it is clear that E_z^{TM} is proportional to $\cos((q\pi z)/(d))$. Likewise, since $A = -B$ for the TE modes, it is clear that H_z^{TE} is proportional to $\sin((q\pi z)/(d))$. It then follows that the solution in (20) corresponds to the TM polarization, which is proportional to the cosine function. To create a corresponding solution for the TE polarization that is proportional to the sine function, the solution in (20) needs to have a phase offset of $-\pi/2$ added to the argument of the cosine.

C. Closed Form for the Eigenfrequencies

The WKB solution will now be applied to the truncated conical resonator to find its resonant frequencies. As described in Section III-C, in order to satisfy the boundary conditions at the end cap at $z = d$, the argument of the cosine function in (20) (for TM field solutions—the TE solutions are governed by the sine function), must be an integer multiple of π when $z = d$. However, by convention in the spherical coordinate system, the first index value of the radial index q in the conical resonator is one, not zero (i.e., $q = 1, 2, 3, \ldots$) [1]. To account for this convention, one needs to add a factor of π to the argument of the cosine in (20) (in addition to the factor of $-\pi/2$ for the TE polarizations). Thus, the overall factor for the TM modes is $+3\pi/4$ and for the TE modes is $+\pi/4$. Letting the argument of the cosine in (20) for $x > x_0$ be $\Phi(z)$ and replacing $f(x)$ with $k_z^2(z)$ (i.e., the squared waveguide propagation constant) and x_0 by z_c (i.e., the turning point), the concise resonance condition can be written as follows:

$$\Phi(z = d) = \int_{z_c}^{d} k_z(z')dz' + \vartheta = q\pi$$
$$\vartheta = \begin{cases} \pi/4 \rightarrow \mathrm{TE} \\ 3\pi/4 \rightarrow \mathrm{TM} \end{cases} \tag{28}$$

where $q = 1, 2, 3, \ldots$, and the variable ϑ selects the appropriate phase value corresponding to the TM and TE field solutions, as discussed previously. Substituting $k_z(z)$, as defined in (23) into (28), gives

$$\Phi(z = d) = \int_{z_c}^{d} \sqrt{k^2 - \left(\frac{x_{np}}{a_0 + z'\tan\theta_c}\right)^2} dz' + \vartheta = q\pi. \tag{29}$$

An evaluation of the integral in the above expression is now required. Rewriting and letting $\alpha = x_{np}/k\tan\theta_c$ and $\beta = a_0/\tan\theta_c$, the integral can be written as

$$\int_{z_c}^{d} k\sqrt{1 - \left(\frac{x_{np}}{k\tan\theta_c}\right)^2 \left(\frac{1}{\frac{a_0}{\tan\theta_c} + z'}\right)^2} dz' = \int_{z_c}^{d} k\sqrt{1 - \alpha^2\left(\frac{1}{\beta + z'}\right)^2} dz'. \tag{30}$$

Changing variables to let $\gamma = \beta + z'$, the integral becomes

$$\int_{\beta+z_c}^{\beta+d} k\sqrt{1 - \alpha^2\left(\frac{1}{\gamma^2}\right)} d\gamma = \int_{\beta+z_c}^{\beta+d} \frac{k}{\gamma}\sqrt{\gamma^2 - \alpha^2} d\gamma. \tag{31}$$

The above integral can be solved using trigonometric substitution, letting $\gamma = \alpha\sec\varphi$, thus $d\gamma = \alpha\sec\varphi\tan\varphi d\varphi$,

$$k\int_{\varphi_c}^{\varphi_d} \frac{\sqrt{\alpha^2\sec^2\varphi - \alpha^2}}{\alpha\sec\varphi} \alpha\sec\varphi\tan\varphi d\varphi = k\alpha\int_{\varphi_c}^{\varphi_d} \tan^2\varphi d\varphi = \frac{x_{np}}{\tan\theta_c}[\tan\varphi - \varphi]_{\varphi_c}^{\varphi_d} \tag{32}$$

where φ_c corresponds to the point $z' = z_c$ and φ_d corresponds to the point $z' = d$. Examining the relationship between φ and z', it can be seen that

$$\cos\varphi = \frac{\alpha}{\beta + z'} = \frac{x_{np}/k}{a_0 + z'\tan\theta_c} = \frac{k_\rho(z')}{k}. \tag{33}$$

If we consider the 2-D k space made by k_ρ and k_z, then the magnitude of the k vector at any distance along the z-axis in the conical resonator is $k = \sqrt{k_\rho^2 + k_z^2}$ and the phase angle of that k vector is given by φ. Thus, at $z' = z_c$ (i.e., the radius at which a given mode becomes cutoff and $k_\rho = k$), the phase of the k vector, φ, is zero, and so $\varphi_c = 0$ and $\varphi_d = \cos^{-1}(k_\rho/k) = \cos^{-1}(x_{np}/ka_d)$, where a_d is the radius of the cone at $z' = d$. Substituting φ_c and φ_d into the solution for the integral in (32) and inserting this integral into the resonance condition given in (28), the closed-form solution of the resonance condition is obtained as follows:

$$\frac{x_{np}}{\tan\theta_c}[\tan\varphi_d - \varphi_d] + \vartheta = q\pi \quad \vartheta = \begin{cases} \pi/4 \rightarrow \mathrm{TE} \\ 3\pi/4 \rightarrow \mathrm{TM} \end{cases} \tag{34}$$

where $\varphi_d = \cos^{-1}(x_{np}/ka_d)$ and $k = \omega\sqrt{\mu\epsilon}$. Even though this expression still requires a transcendental solution to find the allowable wavenumbers k (and thereby the resonant frequencies ω) corresponding to the TE_{npq} or TM_{npq} mode triplets, it is simple and can be solved using much less demanding methods than the transcendental solutions involving the Legendre functions and spherical Bessel functions of noninteger order. One is only required to look up the zeros of the cylindrical Bessel function (x_{np} for the TM modes) and its derivative (x'_{np} for the TE modes) in a table such as [7]. Unlike the solutions using the Legendre and Bessel functions, which assumed spherical end caps on the conical resonator, this solution assumes that the resonator has flat end caps, suggesting that the resonant frequency estimates might be more representative of the actual resonances in the cone.

It is important to note that as higher order modes are considered within a given x_{np} (or x'_{np}) mode family (i.e., increasing index q), there is a frequency beyond which modes do not cutoff before reaching $z = 0$. That is, for those modes with a wavenumber $k > k_\rho(z = 0) = x_{np}/a_0$ and equivalently a resonant frequency $f > (x_{np})/(2\pi\sqrt{\mu\epsilon}a_0)$, the limits of the integral solution in (32) are no longer valid, and therefore, (34) cannot be used. As these discussions focus on the lower order modes, solutions to resonant frequencies higher than the above-stated boundary will not be presented.

Recall that the WKB solution made the assumption in (19) in order for the approximations to be accurate. It is useful to know what this restriction is in terms of the quantities of the derived transcendental solution. We can write the derivative of the function $f(z) = k_z^2(z)$ as follows using the definition given in (23):

$$\frac{df(z)}{dz} = \frac{-2x_{np}^2\tan\theta_c}{(a_0 + z\tan\theta_c)^3}. \tag{35}$$

The approximation inequality follows, substituting in the above derivative of the function and the function itself from (23) into (19) and simplifying

$$\tan\theta_c \ll x_{np}|\tan\varphi|^3 \quad -\frac{\pi}{2} \le \varphi \le \frac{\pi}{2}. \tag{36}$$

Several qualifications can be noticed from the restriction given concisely in (36). The WKB approximation provides adequate solutions to the wave equation in the conical resonator whose half-cone angle θ_c is small and the solutions are being considered for φ significantly larger than zero. Note that the dispersion angle $\varphi(z) = \cos^{-1}(k_\rho/k)$ is equal to zero at the turning point of a given propagating mode, and (36) suggests that the WKB method would have inaccurate solutions for these values of φ; however, since φ is a function of z, the inequality of (36) still holds for regions where the radius is considerably larger than the cutoff radius. Even though this condition does not rigorously hold very near the turning point, the resonant frequencies derived from the WKB method are nevertheless very close to the values derived from the roots of the Legendre and Bessel functions, as will be discussed in Section III-D. Lastly, the x_{np} term in the inequality indicates that the WKB approximation should be more accurate for larger values of x_{np}.

TABLE II
PREDICTED AND MEASURED CONICAL CAVITY RESONANT FREQUENCIES

Mode	Classical Method	WKB	VNA
TE_{011}	800.63 MHz	802.62	N/A
TE_{012}	920.17 MHz	924.03	N/A
TE_{111}	433.50 MHz	433.76	436.06
TE_{112}	535.56 MHz	537.35	538.00
TE_{113}	627.71 MHz	630.50	630.31
TE_{211}	659.37 MHz	659.94	662.69
TE_{212}	772.85 MHz	775.13	775.56
TE_{213}	873.17 MHz	876.52	872.69
TM_{011}	465.92 MHz	471.11	462.31
TM_{012}	593.31 MHz	596.59	594.00
TM_{013}	694.38 MHz	698.39	695.06
TM_{111}	718.24 MHz	724.90	714.31
TM_{112}	862.10 MHz	866.36	864.81
TM_{113}	973.26 MHz	978.21	972.44

D. Comparison of WKB Method to Legendre/Bessel Root Method and Measured Results

Measurements were taken on the conical resonator shown in Fig. 1 using a VNA, as described previously. Table II lists some of the lowest order resonant frequencies below 1.00 GHz of the conical resonator, as determined by the Legendre and Bessel function roots, the WKB method and measurements using the VNA. One can see that the WKB method matches to both the measured and root-derived resonant frequencies very well, often showing a match that is better than 1%. The measured resonant frequencies for the TE_{01p} modes are not listed here since these measurements were made using a linear probe antenna, inserted radially through the cone surface, and this type of antenna will not couple to the TE_{01p} mode family in that position.

It should also be mentioned that both the WKB solution and the Legendre/Bessel root solution require approximations. The WKB method correctly assumes that the conical resonator has flat end caps, but it is itself an approximation to the dispersion relationship, and thus, the resonant frequencies. The Legendre/Bessel Root method assumes that the conical resonator has spherically-shaped end caps (an approximation), but finds exact resonant frequency solutions under that assumption. It is not clear, however, from Table II that one of these methods is clearly more accurate than the other, although both methods

do predict the measured values very well. Manufacturing tolerances and geometric imperfections could also be cited for minor deviations from theory in the measured results.

A numerical finite-element method (FEM) or other similar tools could also be used to obtain the resonant frequencies of the truncated conical resonator. Such tools can require the user to specify a minimum solution frequency and the number of modes that the user wishes to obtain above the specified frequency. The transcendental solution described in this paper allows the user to quickly solve for the eigenfrequency of interest in order to cue an FEM or similar tool to find potentially more accurate solutions. This ability to effectively narrow the solution space would be particularly useful in overmoded resonators, as it may be impractical to solve for every resonant mode from the fundamental mode extending to the mode of interest. However, such FEM solutions would almost certainly take longer than the computationally inexpensive solution presented in (34).

IV. Conclusion

The WKB method is applied here to obtain the solution of the eigenfrequencies of a conical cavity resonator. While the solution using the WKB method is approximate, it contains only simple trigonometric functions, distinct from the classical boundary value method that requires more complex noninteger degrees of the Legendre functions and noninteger order Bessel functions in order to find the cavity's eigenfrequencies. The match observed between the WKB approximation and the classical boundary value problem is very good. Such good agreement along with the simplicity of the WKB solution makes it a very attractive method for finding the eigenfrequencies of a conical cavity resonator. Experimental results agree well with both the classical method and the WKB method.

References

[1] R. F. Harrington, *Time–Harmonic Electromagnetic Fields*. New York: Wiley, 2001.

[2] J. P. Van't Hof and D. D. Stancil, "Characterizing dispersion in the enclosed-space radio channel using a composite mode model," in *Proc. IEEE/ACES Int. Wireless Commun. Appl. Comput. Electromagn. Conf.*, 2005, pp. 818–823.

[3] J. P. Van't Hof and D. D. Stancil, "Dispersion in the enclosed-space radio channel: Measurements and model," in *Proc. IEEE AP-S Int. Symp.*, 2005, vol. 3B, pp. 225–228.

[4] J. P. Van't Hof and D. D. Stancil, "Wireless sensors in reverberant enclosures: Characterizing a new radio channel," in *Proc. IEEE 62nd Veh. Technol. Conf.*, 2005, vol. 3, pp. 1747–1750.

[5] J. P. Van't Hof, "Modeling the dispersion and gain of RF wireless channels inside reverberant enclosures," Ph.D. dissertation, Dept. Elect. Comput. Eng., Carnegie Mellon Univ., Pittsburgh, PA, 2005.

[6] B. Mayer, R. Knöchel, and A. Reccius, "Novel truncated cone cavity for surface resistance measurements of high T_c superconducting thin films," in *Proc. IEEE MTT-S Int. Microw. Symp. Dig.*, Jun. 1991, vol. 3, pp. 1019–1022.

[7] M. Abramowitz and I. A. Stegun, *Handbook of Mathematical Functions*, 9th ed. New York: Dover, 1972.

[8] S. Schelkunoff, *Electromagnetic Waves.*. Princeton, NJ: Van Nostrand, 1943.

[9] J. Mathews and R. Walker, *Mathematical Methods of Physics*, 2nd ed. Menlo Park, CA: W. A. Benjamin, 1970.

[10] H. Jeffreys and B. Jeffreys, *Methods of Mathematical Physics*. New York: Cambridge Univ. Press, 1966.

[11] H. Kramers, "Wellenmechanik und halbzahlige quantisierung," *Z. Phys.*, vol. 39, pp. 828–840, 1926.

[12] N. Matuschek, F. X. Kartner, F. X. Kartner, U. Keller, and U. Keller, "Theory of double-chirped mirrors," *IEEE J. Sel. Topics Quantum Electron.*, vol. 4, no. 2, pp. 197–208, Feb. 1998.

[13] Y. C. E. Yang and Q. Gu, "Time-domain perturbational analysis of nonuniformly coupled transmission lines," *IEEE Trans. Microw. Theory Tech.*, vol. MTT-33, no. 11, pp. 1120–1130, Nov. 1985.

[14] J. W. Silvestro, R. E. Collin, and R. E. Collin, "Aperture impedance of flared horns," *Proc. Inst. Elect. Eng.—Microw., Antennas, Propag.*, vol. 136, no. 3, pt. H, pp. 235–240, 1989.

[15] P. J. B. Clarricoats, S. M. Tun, and C. G. Parini, "Effects of mutual coupling in conical horn arrays," *Proc. Inst. Elect. Eng.—Microw., Opt., Antennas*, vol. 131, pt. H, pp. 165–171, 1984.

[16] N. Amitay and M. J. Gans, "Design of rectangular horn arrays with oversized aperture elements," *IEEE Trans. Antennas Propag.*, vol. AP-29, no. 6, pp. 871–884, Nov. 1981.

Jonathan P. Van't Hof (S'98–M'05) received the B.S., M.S., and Ph.D. degrees in electrical and computer engineering from Carnegie Mellon University, Pittsburgh, PA, in 2000, 2001, and 2005, respectively.

From 2001 to 2005, he was a Graduate Research Assistant with Sandia National Laboratories, Livermore, CA. In 2005, upon completion of the doctoral degree, he joined the Applied Physics Laboratory, The Johns Hopkins University, Laurel, MD. His research interests include wireless communications, radar, and other RF systems.

Daniel D. Stancil (S'75–M'81–SM'91–F'03) received the B.S. degree in electrical engineering from Tennessee Technological University, Cookeville, in 1976, and the S.M., E.E., and Ph.D. degrees from the Massachusetts Institute of Technology (MIT), Cambridge, in 1978, 1979, and 1981, respectively.

From 1981 to 1986, he was Assistant Professor of electrical and computer engineering with North Carolina State University, Raleigh. In 1986, he joined the faculty of Carnegie Mellon University (CMU), Pittsburgh, PA, as an Associate Professor, and is currently a Professor. From 1992 to 1994, he was Associate Department Head of the Department of Electrical and Computer Engineering, CMU. From 1996 to 2000, he served as Associate Dean for Academic Affairs of the College of Engineering, CMU. In 1996, he co-founded the Applied Electro-optics Corporation. He was a leader in the development of the Virtual Laboratory, Department of Electrical and Computer Engineering, CMU. His research interests include wireless communications and optical data storage.

Dr. Stancil was the recipient of a 1985 Sigma Xi Research Award presented by North Carolina State University. CMU's Virtual Laboratory was a finalist for a 1996 Smithsonian Computerworld Award. He was the corecipient of a 1998 Science Award for Excellence presented by the Pittsburgh Carnegie Science Center, a Research and Development 100 Award, and a Photonics Circle of Excellence Award for the development and commercialization of electrooptic technology.